Genesis of the Lengshuikeng Pb-Zn Deposit, China: Constraint from In-situ LA-ICP-MS Analyses of Minor and Trace Elements in Sphalerite

Xuejing Gong, Qingtian Lü, Guixiang Meng, Jiayong Yan and Jinhua Zhao

Sinoprobe Center, Chinese Academy of Geological Science
No 26, Baiwanzhuang Road, Beijing, 100037, China
Email:xuejinggong@cags.ac.cn

SUMMARY

It is generally believed that at medium and low temperature, Pb and Zn are still difficult to precipitate and form porphyry mineralization due to the high solubilities. However, the Lengshuikeng deposit in Jiangxi Province is considered to be a porphyry lead-zinc deposit according to the close temporal and spatial relationship between Pb-Zn mineralization and the granite porphyries. To check the metal source of the Lengshuikeng deposit, we investigated the sphalerite using in situ analysis techniques (LA-ICP-MS, EMPA), to constrain the metal source and the mineralization temperature. The analysis results suggest that the Lengshuikeng deposit is a kind of hydrothermal deposits which formed in middle-low temperature environment and the ore-forming material dominantly comes from the porphyry magma system.

Key words: Sphalerite, Trace elements, LA-ICP-MS, Pb-Zn deposit, Southeast China

INTRODUCTION

The porphyry mineral system usually consists of porphyry deposits, proximal skarn deposits, distal stratabound deposits, and epithermal deposits(Sillitoe., 2010). It has been shown that the porphyry copper-molybdenum-gold deposits are closely related to magma properties and sources(Hedenquist et al., 1998; Richards, 2003; Cooke et al., 2005; Hou et al., 2004,2007,2012; Hou and Yang., 2009; Zhang et al., 2009), but the genesis correlation between lead-zinc deposits and porphyry magma system is still not clear. Therefore, further research on the genetic of lead-zinc mineralization in porphyry system has significant scientific and production value.

The Lengshuikeng lead-zinc deposit in Jiangxi Province is one of the largest porphyry-related Pb-Zn deposits in the North Wuyi metallogenic belt in China, the ore reserves have been estimated at ~43Mt with average grades of 2.11% Pb, 2.61% Zn, 204.53g/t Ag, 0.08g/t Au, and 0.01% Cd. The Lengshuikeng deposit consists of two main orebodies: the porphyry-hosted and the stratabound, and is related to a 162Ma, most buried mushroom-shaped stock of granite porphyry(Figure.1) spatially and temporally. However, the genesis of the two kinds of ore bodies and their relationship remain controversial.

Sphalerite is the main ore-forming mineral in lead-zinc deposits, and contains trace elements such as Fe, Mn, Cd, Ga, Ge, In, Se, Te. The contents of these characteristic elements is often used in discriminating the genesis of lead-zinc deposits and tracking mineralization information (Claussen, 1934; Graton and Harcourt, 1935; Stoiber, 1940; Zhang, 1987; Di Benedetto et al., 2005; Monteiro et al., 2006; Gottesmann and Kampe, 2007; Wang et al., 2010). With the emergence of LA-ICP-MS high-precision instruments and the maturity of in-situ sulfide trace element testing techniques, some researchers have applied this method to the study of deposits genesis, providing a ladder for revealing the ore-forming process(Cook et al., 2009,2011; Ye et al., 2011, 2012; Belissont et al., 2014, 2016; Wohlgemuth-Ueberwasser et al., 2015; Xing et al., 2016). In this study, the LA-ICP-MS test technique was used to study the characteristics of trace elements in both the porphyry-hosted and the stratabound ore bodies in Lengshuikeng deposit, which directly restricted the source of metals and further constrained the formation temperature.

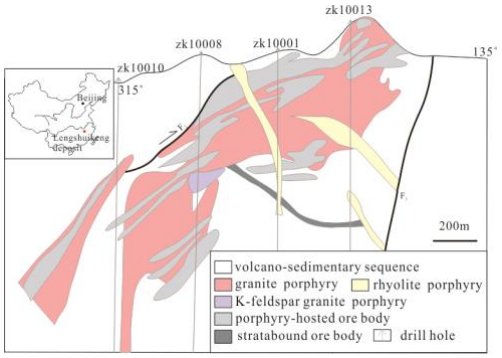

Figure 1. Geologic map of No. 132 cross in Lengshuikeng Pb-Zn deposit (modified after Wang et al., 2014).

METHOD AND RESULTS

Based on detailed field geological survey and microscopic identification, we conducted electron microprobe and laser ablation plasma mass spectrometry analysis on both the porphyry-hosted and the stratabound mineralized samples in Lengshuikeng deposit. The electronic microprobe analysis(EPMA) was completed on a JEOL-JXA-8230 in the Institute of Mineral Resources, CAGS, with acceleration voltage of 15kV, current of 20nA and beam spot of 5μm. Laser ablation-inductively coupled plasma-mass spectrometry (LA-ICP-MS) analysis was carried out in Wuhan Shangpu Analysis Technology Co., Ltd. The Agilent HP-7700 Quadripole ICPMS was connected using a 193 nm laser ablation system with a beam spot diameter of 32 μm. The analysis results was calibrated with both internal and external standards. The internal standard was EPMA results of Zn, and the external standards were NIST610 and MASS-1. The ICPMS DataCal

(Liu et al., 2008) was used to process the sample signal and calculate the test values, errors and detection limits. According to the judgment of the detection limit, effective data of elements such as P, S, Ti, Mn, Fe, Cu, Zn, Ga, Ge, As, Ag, Cd, In, Sn, Sb and Pb were obtained.

EPMA and LA-ICP-MS analysis results are listed in Table 1 and Table 2 respectively. We analyzed two porphyry-hosted ore samples at 18 testing points on sphalerite. The composition of the porphyry-hosted ore samples shows the following characteristics: The contents of Cd are relatively high, which range from 1085.67×10^{-6} to 2305.01×10^{-6}, with an average of 1720.51×10^{-6} (n=18). The content of Cu and Pb varied widely, the range of Cu varied from 11.10×10^{-6} to 6004.05×10^{-6} and the range of Pb varied from 44.37×10^{-6} to 132251.23×10^{-6}. The sphalerite is enriched in Mn (460.12×10^{-6}~11343.52×10^{-6}), but depleted in In (0.19×10^{-6}~5.73×10^{-6}), Ge (0.68×10^{-6}~7.58×10^{-6}), Ga(3.07×10^{-6}~10.59×10^{-6}) and Sn (15.92×10^{-6}~1356.67×10^{-6}). In addition, contents of As, Co, Ni and Sr are extremely low, and most of the results are below the detection limit.

25 points were analysed on sphalerite in 4 stratabound ore samples, and the trace element composition characteristics were generally consistent with porphyry-hosted samples: Cd contents were concentrated between 2604.86×10^{-6} and 4509.19×10^{-6}, with an average of 3363.93×10^{-6} (n = 25). The content of Cu and Pb varied widely also, the range of Cu varied from 15.28×10^{-6} to 3706.57×10^{-6} and the range of Pb varied from 1.82×10^{-6} to 117665.74×10^{-6}. The sphalerite is relatively enriched in Mn (62.11×10^{-6}~1217.03×10^{-6}) and In (0.35×10^{-6}~765.09×10^{-6}), but depleted in Ge (0.45×10^{-6}~3.44×10^{-6}), Ga (0.02×10^{-6}~3.72×10^{-6}) and Sn (13.68×10^{-6}~316.28×10^{-6}).

It can be seen from the comparison that the porphyry-hosted ore body has higher Cu, Mn, Ge, Ga, Sn contents and lower Cd, Pb, In contents than the stratabound ore body. It is worth noting that in the LA-ICP-MS time resolution profile(Figure. 2a), the Cu and Pb in all samples show irregular curves with large variations. It is consistent with the presence of a large number of "chalcopyrite viruses" (Figure. 2b) in sphalerite, indicating that the presence of individual abnormal high values of Cu and Pb may be caused by the chalcopyrite and galena inclusions in sphalerite.

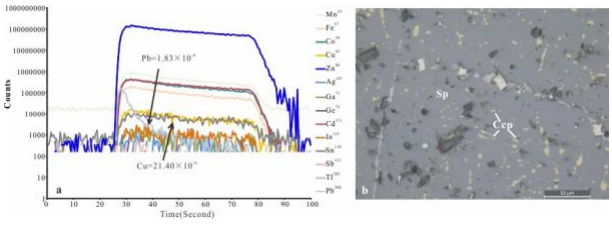

Figure 2. a-Representative time-resolved depth profiles for sphalerite analysed by LA-ICP-MS and b-Microphoto of 'chalcopyrite viruses' in sphalerite.

CONCLUSIONS

The analytical results show an enrichment of Fe, Cd, Mn and a depletion of In, Ga, Ge, Sn, the contents of Cu and Pb various widely with some abnormally high point which due to the chalcopyrite and galena inclusions in the sphalerites. The log (Ga/Ge) values of the sphalerite in the stratabound ore body in Lengshuikeng ranges from -2.47 to 0.89(-0.45 as average), and the log (Ga/Ge) values of the sphalerite in the porphyry-hosted ore body ranges from 0.37 to 1.11(0.73 as average). According to the log(Ga/Ge)-t temperature empirical diagram(Möller, 1987), the spectulated formation temperature is 100 ℃~240 ℃(130 ℃ as average) for stratabound ore body and 210℃~250℃(220 ℃ as average) for porphyry-hosted ore body(Figure. 3a). The Zn/Cd values of the sphalerite in the stratabound ore body and porphyry-hosted ore body are 126.55~230.65(160.94 as average) and 285.80~494.30 (354.90 as average), respectively. These results indicate that the deposit is a kind of hydrothermal deposits which formed in a middle-low temperature environment, and the formation temperature of porphyry-hosted ore body is slightly higher than stratabound ore body.

The values and discriminant diagram(Figure. 3b) of the characteristic elements in the analyzed sphalerites show that the formation of stratabound and porphyry-hosted ore body in Lengshuikeng deposit are mainly controlled and influenced by magmatic hydrothermal action. In summary, we suggest that the two types of ore bodies in the Lengshuikeng deposit have an identical genetic mechanism, with ore-forming material dominantly comes from the porphyry magma system.

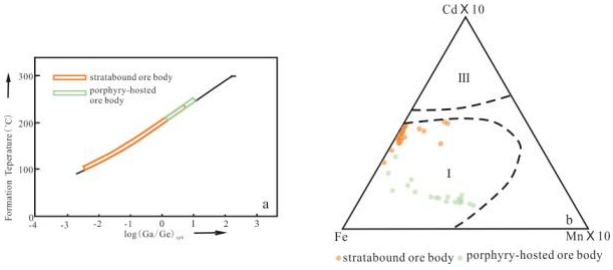

Figure 3. a-Schematic diagram of empirical temperature estimation for sphalerite formation in Lengshuikeng Pb-Zn deposit (according to Möller, 1987); b- Discriminant diagram of Fe-Cd-Mn formation in sphalerite in Lengshuikeng Pb-Zn deposit(Ⅰ-magmatic-hydrothermal deposit； Ⅲ-sedimentary modified deposit, according to Zhang, 1987).

ACKNOWLEDGMENTS

We are grateful to the staff of the No.912 Geological Party of Jiangxi Bureau of Geology and Minerals Exploration for their support in the field work. This study is supported by the National Natural Science Foundation of China under Grant 41802097.

REFERENCES

Belissont, R., Boiron, M., Luais, B. and Cathelineau, M., 2014, LA-ICP-MS analyses of minor and trace elements and bulk Ge isotopes in zoned Ge-rich sphalerites from the Noailhac-Saint-Salvy deposit (France): Insights into incorporation mechanisms and ore deposition processes, Geochimica et Cosmochimica Acta, 126, 518-540.

Belissont, R., Munoz, M., Boiron, M. C., Luais, B. and Mathon, O., 2016, Distribution and oxidation state of Ge, Cu and Fe in sphalerite by μ-XRF and K-edge μ-XANES: insights into Ge incorporation, partitioning and isotopic fractionation, Geochimica et Cosmochimica Acta, 177, 298-314.

Claussen, G. E., 1934, Spectroscopic analysis of certain galenas, sphalerites, and pyrites, American Mineralogist, 19, 221-224.

Cook, N. J.， Ciobanu, C. L., Pring, A., Skinner, W., Shimizu, M., Danyushevsky, L., Saini-Eidukat, B. and Melcher, F., 2009, Trace and minor elements in sphalerite: A LA-ICP-MS study, Geochimica et Cosmochimica Acta, 73, 4761-4791.

Cook, N. J., Ciobanu, C. L. and Williams, T., 2011. The mineralogy and mineral chemistry of indium in sulphide deposits and implications for mineral processing[J]. Hydrometallurgy, 108(3-4): 226-228.

Cooke, D. R., Holling, P. and Walshe, J. L., 2005, Giant porphyry deposits: Characteristics, distribution, and tectonic controls, Economic Geology, 100, 801-818.

Di Benedetto, F., Bernardini, G. P., Costagliola, P., Plant, D. and Vaughan, D. J., 2005, Compositional zoning in sphalerite crystals, American Mineralogist, 90: 1384-1392.

Gottesmann, W. and Kampe, A., 2007, Zn /Cd ratios in calcsilicate-hosted sphalerite ores at Tumurtijn-ovoo, Mongolia, Chemie der Erde, 67: 323-328.

Graton, L. C. and Harcourt, G. A., 1935, Spectrographic evidence on origin of ores of Mississippi Valley type, Economic Geology, 30(7), 800-824.

Hedenquist, J. W., Arriba, A. J. and Reynolds, T. J ., 1998, Evolution of an intrusion-centered hydrothermal system: Far Southeast-Lepanto porphyry and epithermal Cu-Au deposits, Philippines, Economic Geology, 93, 373-404.

Hou, Z. Q., Gao, Y. F., Meng, X. J., Qu, X. M. and Huang, W., 2004, Genesis of adakitic porphyry and tectonic controls on the Gangdese Miocene Porphyry copper belt in the Tibetan orogeny, Acta Petrologica Sinica, 20(2), 239-248(in Chinese with English abstract).

Hou, Z. Q., Pan, X. F., Yang, Z. M. and Qu, X. M., 2007, Porphyry Cu-(Mo-Au) deposits not related to oceanic-slab subduction: Examples from Chinese porphyry deposits in continental settings, Geoscience, 21:332-351(in Chinese with English abstract).

Hou, Z. Q. and Yang, Z. M., 2009, Porphyry deposits in continental settings of China: Geological characteristics, magmatic-hydrothermal system, and metallogenic model, Acta Geologica Sinica, 83(12),1780-1817(in Chinese with English abstract).

Hou, Z. Q., Zheng, Y. C., Yang, Z. M. and Yang, Z. S., 2012, Metallogenesis of continental collision setting: Part I . Gangdese Cenozoic porphyry Cu-Mo system in Tibet, Mineral Deposits, 31(4): 647-670(in Chinese with English abstract).

Liu, Y. S., Hu, Z. C., Gao, S., Gunther, D., Xu, J., Gao, C. G. and Chen, H. H., 2008, In situ analysis of major and trace elements of anhydrous minerals by LA-ICP-MS without applying an internal standard, Chemical Geology, 257(1-2), 34-43.

Möller, P., 1987, Correlation of homogenization temperatures of accessory minerals from sphalerite-bearing deposits and Ga/Ge model temperatures. Chemical geology, 61(1), 153-159.

Monteiro, L. V. S., Bettencourt, J. S., Juliani, C. and Oliveira, T. F. D., 2006, Geology, petrography, and mineral chemistry of the Vazante non-sulfide and Ambro'sia and Fagundes sulfide-rich carbonate-hosted Zn-(Pb) deposits, Minas Gerais, Brazil, Ore Geology Reviews, 28, 201-234.

Richards, J. P ., 2003, Tectono-magmatic precursors for porphyry Cu-(Mo-Au) deposit formation, Economic Geology, 98, 1515-1533.

Sillitoe, R. H., 2010, Porphyry copper systems, Economic Geology, 105(1), 3-41.

Stoibe,r R. E., 1940, Minor elements in sphalerite, Economic Geology, 35(4), 501-519.

Wang, C. M., Deng, J., Zhang, S. T., Xue, C. J., Yang, L. Q., Wang, Q. F. and UN, X., 2010, Sediment-hosted Pb-Zn deposits in Southwest Sanjiang Tethys and Kangdian area on the western margin of Yangtze Craton, Acta Geologica Sinica(English Edition), 84(6), 1428-1438.

Wang, C. M., Zhang, D., Wu, G. G., Santosh, M., Zhang, J., Xu, Y. G., and Zhang, Y. Y., 2014, Geological and isotopic evidence for magmatic-hydrothermal origin of the Ag-Pb-Zn deposits in the Lengshuikeng District, east-central China. Miner Deposita, 49, 733-749.

Wohlgemuth-Ueberwasser, C. C., Viljoen, F., Petersen, S. and Vorster, C., 2015, Distribution and solubility limits of trace elements in hydrothermal black smoker sulfides: An in-situ LA-ICP-MS study, Geochimica et Cosmochimica Acta, 159, 16-41.

Xing, B., Zheng, W., Ouyang, Z. X., Wu, X. D., Lin, W. P. and Tian, Y., 2016, Sulfide microanalysis and S isotope of the Miaoshan Cu polymetallic deposit in western Guangdong Province, and its constraints on the ore genesis, Acta Geologica Sinica, 05, 971-986(in Chinese with English abstract).

Ye, L., Cook, N. J., Ciobanu, C. L., Liu, Y. P., Zhang, Q., Liu, T. G., Gao, W., Yang, Y. L. and Danyushevskiy, L., 2011, Trace and minor elements in sphalerite from base metal deposits in South China: A LA-ICPMS study, Ore Geology Reviews, 39(4), 188-217.

Ye, L., Gao, W., Yang, Y. L., Liu, T. G. and Peng, S. S., 2012, Trace elements in sphalerite in Laochang Pb-Zn polymetallic deposit, Lancang, Yunnan Province, Acta Petrologica Sinica, 28(5), 1362-1372(in Chinese with English abstract).

Ye, L., Li, Z. L., Hu, Y. S., Huang, Z. L., Zhou, J. X., Fan, H. F. and Danyushevskiy, L., 2016, Trace elements in sulfide from the Tianbaoshan Pb-Zn deposit, Sichuan Province, China: A LA-ICPMS study, Acta Petrologica Sinica, 32(11), 3377-3393(in Chinese with English abstract).

Zhang, H. R., Hou, Z. Q., Song, Y. C., Li, Z., Yang, Z. M., Wang, Z. L., Wang, X. H. and Wang, S. X., 2009, The temporal and spatial distribution of porphyry copper deposits in the eastern Tethyan metallogenic domain: A review, Acta Geologica Sininca, 83(12), 1818-1837(in Chinese with English abstract).

Zhang, Q., 1987, Trace elements in galena and sphalerite and their geochemical significance in distinguishing the genetic types of Pb-Zn ore deposits, Geochemistry, 6(2), 177-190.

Hendrick, N., and Hearn, S., 1999, Polarisation analysis: What is it? Why do you need it? How do you do it?: Exploration Geophysics, 30, 177-190.

Table1 Electron microprobe analysis(EPMA) results for sphalerite from Lengshuikeng Pb-Zn deposit, China

No.	Fe	S	Ni	Se	As	Ge	Pb	Bi	Cu	Zn	Co	Sb	Total
PD11501-4-1	6.15	34.24	0.00	0.03	0.00	0.00	0.02	0.00	0.02	60.22	0.02	0.00	100.69
PD11501-4-2	4.75	33.52	0.00	0.00	0.00	0.00	0.03	0.04	0.00	63.43	0.01	0.00	101.77
PD11501-4-3	10.44	33.71	0.01	0.02	0.03	0.00	0.01	0.00	0.02	56.33	0.02	0.00	100.57
PD11501-4-4	7.62	33.87	0.02	0.00	0.04	0.00	0.11	0.00	0.00	58.43	0.01	0.00	100.11
PD11501-4-5	9.07	33.90	0.00	0.03	0.00	0.00	0.04	0.00	0.06	58.25	0.00	0.03	101.38
PD11501-4-6	8.98	33.95	0.01	0.01	0.00	0.00	0.00	0.00	0.00	58.35	0.00	0.00	101.30
PD11501-4-7	8.77	33.30	0.00	0.00	0.01	0.00	0.02	0.00	0.00	57.03	0.00	0.01	99.14
PD11501-4-8	12.48	33.90	0.00	0.00	0.09	0.03	0.00	0.00	0.02	53.28	0.02	0.00	99.82
PD11501-4-9	9.46	33.92	0.00	0.00	0.00	0.00	0.00	0.00	0.04	58.31	0.03	0.01	101.76
PD11501-4-10	10.56	34.11	0.00	0.02	0.00	0.01	0.00	0.00	0.23	56.19	0.01	0.00	101.13
PD11501-4-11	7.97	33.81	0.01	0.00	0.00	0.00	0.00	0.00	0.03	59.83	0.02	0.00	101.68
PD11501-4-12	10.77	33.78	0.02	0.00	0.00	0.04	0.00	0.00	0.91	55.54	0.02	0.00	101.07
PD11501-4-13	11.13	33.99	0.00	0.00	0.05	0.00	0.14	0.00	0.00	56.04	0.02	0.00	101.37
PD11501-4-14	13.28	33.96	0.00	0.03	0.00	0.00	0.00	0.01	0.00	54.78	0.02	0.02	102.11
PD11501-4-15	11.52	33.85	0.00	0.03	0.00	0.00	0.12	0.00	0.30	55.43	0.03	0.00	101.27
PD11501-4-16	8.96	32.75	0.00	0.00	0.00	0.00	0.02	0.00	0.29	57.31	0.05	0.00	99.39
PD11501-4-17	4.41	32.67	0.02	0.00	0.00	0.00	0.07	0.04	0.00	61.75	0.00	0.00	98.95
PD11501-4-18	10.39	32.79	0.01	0.00	0.05	0.01	0.00	0.00	0.18	55.50	0.03	0.00	98.94
XB122-3-1	8.48	34.42	0.00	0.00	0.00	0.00	0.01	0.00	0.01	58.00	0.00	0.00	100.92
XB122-3-2	8.01	33.07	0.00	0.00	0.00	0.00	0.00	0.00	0.03	59.47	0.03	0.00	100.61
XB122-3-3	8.56	34.14	0.02	0.00	0.03	0.00	0.00	0.00	0.58	58.42	0.03	0.01	101.79
XB122-3-4	7.35	34.39	0.03	0.00	0.00	0.04	0.00	0.00	0.02	58.16	0.01	0.02	100.02
XB122-3-5	7.25	32.82	0.00	0.00	0.00	0.00	0.00	0.00	0.01	59.09	0.04	0.00	99.21
XB-TB-2-1	5.21	33.81	0.00	0.00	0.00	0.02	0.07	0.00	0.01	62.64	0.03	0.00	101.79
XB-TB-2-2	5.23	33.76	0.01	0.02	0.00	0.00	0.00	0.00	0.00	62.84	0.04	0.01	101.91
XB-TB-2-3	4.69	33.80	0.01	0.00	0.00	0.00	0.04	0.00	0.11	63.02	0.04	0.02	101.73
XB-TB-2-4	2.98	33.82	0.00	0.00	0.00	0.00	0.00	0.00	0.02	63.19	0.00	0.01	100.02
XB-TB-2-5	3.22	33.69	0.00	0.04	0.00	0.02	0.00	0.00	0.00	63.27	0.00	0.00	100.24
XB122-6-1	10.43	33.95	0.00	0.00	0.00	0.00	0.04	0.00	0.05	57.16	0.04	0.00	101.66
XB122-6-2	7.02	32.09	0.01	0.00	0.03	0.00	0.06	0.00	0.21	57.34	0.02	0.00	96.78
XB122-6-3	8.55	33.07	0.03	0.00	0.01	0.00	0.01	0.02	0.00	56.37	0.03	0.00	98.08
XB122-6-4	7.63	33.22	0.00	0.05	0.04	0.00	0.08	0.00	0.24	59.05	0.02	0.00	100.33
XB122-6-5	5.97	34.00	0.00	0.00	0.20	0.02	0.02	0.00	0.41	61.16	0.01	0.01	101.80
XB210-1-1	9.34	34.46	0.01	0.00	0.06	0.00	0.01	0.00	0.01	60.52	0.02	0.00	104.44
XB210-1-2	9.22	33.40	0.00	0.00	0.00	0.01	0.00	0.00	0.03	58.38	0.03	0.00	101.08
XB210-1-3	9.97	33.74	0.00	0.00	0.00	0.00	0.01	0.00	0.00	57.79	0.03	0.02	101.57
XB210-1-4	8.70	33.65	0.01	0.00	0.02	0.00	0.09	0.00	0.02	57.00	0.01	0.01	99.52
XB210-1-5	9.24	33.94	0.00	0.00	0.01	0.00	0.00	0.19	0.03	56.64	0.03	0.00	100.07
XB210-1-6	9.08	33.41	0.00	0.00	0.00	0.04	0.04	0.00	0.16	58.35	0.00	0.00	101.08
XB210-1-7	9.12	33.57	0.00	0.03	0.02	0.00	0.03	0.00	0.04	58.19	0.02	0.00	101.03
XB210-1-8	9.21	33.58	0.01	0.00	0.00	0.00	0.04	0.00	0.01	57.81	0.03	0.00	100.68
XB210-1-9	9.70	33.55	0.00	0.00	0.00	0.00	0.02	0.00	0.00	58.14	0.03	0.00	101.45
XB210-1-10	9.05	33.69	0.02	0.00	0.02	0.00	0.00	0.03	0.53	58.01	0.04	0.00	101.39

Table2 Trace element analysis(LA-ICP-MS) results for sphalerite from Lengshuikeng Pb-Zn deposit, China

No.	P	Ti	Mn	Cu	Ga	Ge	As	Ag	Cd	In	Sn	Sb	Pb
PD11501-4-1	74.77	2.54	8048.34	11.10	7.40	0.86	0.75	57.99	1854.31	0.35	24.21	4.60	73.73
PD11501-4-2	81.00	4.36	8520.37	4696.53	7.67	1.11	1.18	387.14	1885.50	0.34	32.76	10.08	566.49
PD11501-4-3	65.58	2.49	7801.99	612.19	5.55	1.55	0.42	79.52	1633.40	0.19	17.22	2.42	44.37
PD11501-4-4	58.69	3.16	460.12	6004.05	3.72	0.68	55.79	3805.50	2305.01	1.90	395.70	131.29	126847.31
PD11501-4-5	83.87	3.47	551.32	1439.63	3.45	0.78	35.61	2130.09	1851.61	5.73	1356.67	50.15	132251.23
PD11501-4-6	77.89	2.84	1472.79	75.46	5.15	1.38	14.12	249.48	1646.36	0.43	73.41	94.96	56165.35
PD11501-4-7	56.76	2.99	4395.71	167.77	3.07	1.48	20.65	83.93	1522.68	0.27	16.91	15.34	194.24
PD11501-4-8	57.88	3.39	4385.34	1979.12	8.72	2.22	389.35	166.23	1448.13	0.20	22.11	21.17	220.93
PD11501-4-9	66.46	2.18	6593.30	13.45	8.52	1.00	0.33	70.39	1717.44	0.27	15.92	4.48	104.65
PD11501-4-10	68.24	2.51	7243.32	383.78	7.27	4.57	N/A	1299.08	2089.89	0.58	62.90	15.86	4864.56
PD11501-4-11	64.44	2.50	8215.20	1528.13	10.59	0.73	15.34	764.75	1826.62	0.39	25.60	5.33	92.53
PD11501-4-12	67.31	1.80	3591.07	31.85	4.24	0.79	7.94	129.77	1085.67	0.42	46.22	20.44	698.77
PD11501-4-13	65.10	2.22	7619.14	13.62	8.26	0.96	138.37	197.57	1958.86	0.49	32.12	13.61	138.51
PD11501-4-14	71.11	3.27	2521.94	2528.50	7.64	1.34	14.42	1949.37	1482.39	5.71	1294.45	17.87	1988.49
PD11501-4-15	80.82	3.16	1820.57	799.81	10.23	7.58	11.92	1426.48	1878.17	1.14	198.87	33.78	22547.76
PD11501-4-16	60.81	1.82	1724.23	125.41	9.54	3.62	22.31	526.15	1512.35	1.18	225.21	25.07	2345.70
PD11501-4-17	78.00	3.50	11343.52	649.95	4.56	1.47	2.68	625.98	1923.20	0.78	129.67	6.76	172.04
PD11501-4-18	58.56	3.74	3550.13	28.44	7.19	1.56	6.94	175.74	1347.62	5.23	1172.84	24.48	371.65
XB122-3-1	52.78	2.73	239.08	46.06	0.05	0.73	N/A	4.42	3216.64	42.38	17.43	0.62	12.95
XB122-3-2	49.61	3.57	237.75	236.16	N/A	0.68	N/A	2.88	3262.42	33.24	17.25	0.33	4.66
XB122-3-3	66.03	3.37	72.03	597.62	3.72	0.51	1.53	15.12	3158.62	187.61	51.26	13.12	82.92
XB122-3-4	52.41	3.37	183.59	377.68	0.10	1.10	N/A	6.19	3445.09	119.52	17.80	1.72	58.45
XB122-3-5	71.25	2.73	208.26	128.42	N/A	3.44	N/A	3.96	3411.04	45.86	87.59	0.25	12.89
XB-TB-2-1	58.71	1.51	1024.59	36.62	0.03	N/A	N/A	41.00	2701.57	0.35	15.05	0.17	189.70
XB-TB-2-2	74.90	3.48	766.53	1075.47	N/A	0.63	0.47	644.59	2604.86	1.06	72.55	5.38	24843.41
XB-TB-2-3	60.25	4.38	1217.03	389.16	0.09	N/A	N/A	239.24	2750.41	1.09	18.45	0.66	795.26
XB-TB-2-4	58.92	5.87	620.60	615.89	0.23	0.68	0.83	558.77	2832.79	0.93	40.04	1.19	2137.06
XB-TB-2-5	58.71	N/A	1093.92	15.28	0.04	N/A	N/A	21.78	2648.03	0.61	13.25	0.12	5.03
XB122-6-1	67.13	2.58	125.38	1903.79	0.70	1.14	73.23	30.19	3754.26	187.81	19.74	9.03	95.90
XB122-6-2	55.70	2.38	81.39	1338.05	2.43	0.82	5.68	25.01	3840.64	584.42	24.89	3.22	40.78
XB122-6-3	66.47	1.24	265.30	25.46	0.02	N/A	N/A	4.13	3651.93	20.55	13.68	N/A	1.82
XB122-6-4	75.62	4.79	342.30	453.57	0.04	N/A	N/A	13.41	3523.59	27.14	19.05	1.41	9.19
XB122-6-5	71.62	3.46	296.22	3706.57	2.17	0.73	N/A	10.77	4502.83	41.01	23.45	N/A	7.52
XB210-1-1	86.19	5.07	82.08	1016.69	2.68	1.27	N/A	41.11	4476.51	765.09	316.28	4.74	243.64
XB210-1-2	83.76	2.23	130.81	80.22	0.06	1.08	N/A	9.04	4509.19	94.30	17.54	0.08	2.08
XB210-1-3	65.62	2.09	79.55	663.64	0.25	0.53	N/A	30.76	4313.71	635.21	19.81	7.25	117665.74
XB210-1-4	56.63	2.57	305.39	1037.41	2.54	0.72	N/A	26.45	4037.19	627.65	31.60	1.45	287.93
XB210-1-5	70.31	2.54	62.11	1286.41	0.47	0.67	N/A	31.46	3900.48	521.49	20.32	2.18	44.71
XB210-1-6	81.13	3.04	86.51	640.66	0.51	0.74	N/A	27.06	4132.94	601.92	23.53	1.67	43.31
XB210-1-7	73.39	34.68	210.02	560.55	1.16	0.94	0.48	40.29	4077.15	554.61	42.52	3.86	155.94
XB210-1-8	48.54	2.98	84.50	830.85	0.13	0.93	N/A	18.83	4236.81	548.32	17.19	0.36	13.03
XB210-1-9	93.12	3.29	64.63	1006.27	0.32	0.45	N/A	23.20	4297.62	662.52	17.64	0.67	31.53
XB210-1-10	72.57	2.12	73.76	719.01	1.37	N/A	N/A	20.64	4185.78	531.19	25.28	0.61	15.55